Contribution of energy continuum states to probe absorption signal of atoms in one-dimensional optical molasses

Jun Guo*
Department of Physics, New York University, 4 Washington Place, New York, New York 10003
(Received 7 September 1993)

We present a calculation of the probe absorption spectrum of atoms in a one-dimensional optical molasses formed by a pair of counterpropagating, cross-polarized fields. When the finite angle θ between the propagation direction of a probe field and that of one of the cooling fields is taken into account, we find that, apart from the contributions to the probe absorption signal that are related to the Raman and Rayleigh resonances between the discretized atomic motional states in the molasses direction, there is also a signal arising from the recoil-induced resonances between atomic states with different center-of-mass momenta in the directions transverse to the molasses beams. The magnitudes of these different contributions are compared.

PACS number(s): 32.80.Pj, 42.65.−k

I. INTRODUCTION

When atoms are cooled by a pair of linearly polarized fields with orthogonal polarizations (lin ⊥ lin), the light shifts of the atomic ground-state sublevels are periodically modulated along the laser propagation direction. According to the Bloch's theorem, the energy eigenstates of atoms in this molasses direction possess the same periodicity as the potentials (the Bloch states), whose eigenenergies exhibit bandlike structure. The discretized energy spectra of atoms in one-dimensional (1D) lin ⊥ lin molasses have been observed experimentally through either probe transmission techniques [1] or collection of atomic fluorescence [2]. In both cases, the observed positions and widths of the Raman sidebands in the spectra provide information on the motional energy structure and the degree of spatial localization of atoms in the molasses. The experimental observations agree quantitatively with theoretical calculations based on Bloch-state analysis [3–5].

In the probe transmission spectrum shown in Ref. [1], there also exists a central resonance structure at zero pump-probe detuning, whose shape is sensitive to the probe field polarization direction and which can have a width as narrow as a few KHz. It has been interpreted as originating from Rayleigh resonances within certain motional states, which can also be understood in terms of two-wave mixing processes involving the probe and the pump fields [1,4,6]. The observation of such a narrow line shape is believed to provide the proof of a large-scale spatial order of atoms in the molasses (lattice structure).

The theoretical investigation by Courtois and Grynberg [4] has produced results that are in reasonable agreement with the experiment of Ref. [1]. However, discrepancies between their theory and experiment still exist, especially in regard to the narrow central resonances observed in Ref. [1]. The model adopted in Ref. [4] is strictly one dimensional, in a sense that the probe field propagation direction is chosen to be parallel to the molasses direction. In reality, owing to practical limitations, the probe field propagates at some small but finite angle θ (typically a few degrees) with respect to one of the cooling field. It is the purpose of this paper to show that there can be *additional* contributions to the probe absorption (or transmission) signal when effects related to the nonvanishing angle θ is taken into consideration, and these contributions can become the dominant source to the central resonance line shape under certain conditions.

Generally speaking, if a probe field is sent into the molasses at a small angle θ with respect to one of the cooling (pump) field propagation directions, it is possible that the interference between the probe and this cooling fields leads to the formation of a spatial grating in the direction perpendicular to the molasses, with a grating period given by λ/θ, as illustrated in Fig. 1. Such a grating can be a population grating or a magnetization grating, depending on whether the polarizations of the probe and cooling field are parallel or orthogonal to each other, respectively. Consequently, the cooling field can scatter off such a grating into the probe direction, and the interference between this scattered component and the probe can contribute to the probe transmission sig-

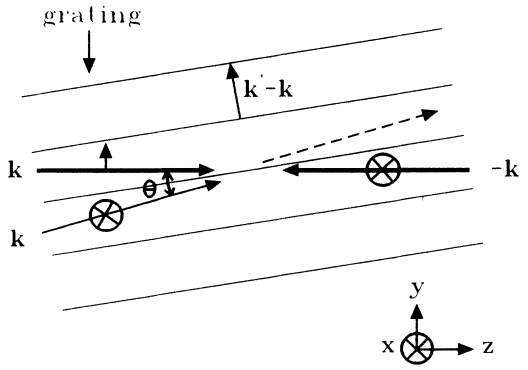

FIG. 1. Transverse grating due to interference between a probe field and a cooling field.

*Present address: Joint Institute for Laboratory Astrophysics, University of Colorado, Boulder, Colorado 80309-0440.

nal. The width of such a signal is determined by the effective relaxation rate of the grating, which corresponds to the residual Doppler dephasing rate $ku\theta$ in the case of a population grating due to atoms moving transverse to the grating with a most probable speed u, or to the optical pumping rate Γ' in the case of a magnetization grating, assuming that $\Gamma' \gg ku\theta$. In the case of a population grating, the signal can be considered as originating from Raman-type processes between the energy continuum states of different atomic c.m. momenta, or the recoil-induced resonances (RIR) [7,8].

To be specific, we consider a case similar to the one treated in Ref. [4], but allowing a small misalignment of the probe field characterized by the angle θ between the propagation directions of the probe and one of the cooling fields. The atomic level scheme is assumed to be a $J_g = 1/2 \rightarrow J_e = 3/2$ transition. The probe absorption coefficient as a function of the probe-pump detuning is calculated. This paper is organized as follows. In Sec. II, we write down the operator equation for the atomic density matrix and derive the expression for the probe absorption coefficient. In Sec. III, we calculate various parts of contributions to the signal and compare the relative magnitudes of these signals under certain conditions. Finally, in Sec. IV, we discuss the relations of our results to some recent experiments.

II. DENSITY MATRIX EQUATION AND THE PROBE ABSORPTION COEFFICIENT

The incident field configuration is shown in Fig. 1. The cooling fields propagate in the positive and negative $\hat{\mathbf{z}}$ directions, with polarizations in the $\hat{\mathbf{y}}$ and $\hat{\mathbf{x}}$ directions, respectively. The probe field propagates at an angle $\theta \in (0,\pi)$ with the $\hat{\mathbf{z}}$ direction, polarized in the $\hat{\mathbf{x}}$ direction. The total field is thus written as

$$\mathbf{E} = \frac{1}{2}(\mathcal{E}\hat{\mathbf{y}}e^{i\mathbf{k}\cdot\mathbf{R}-i\Omega t} + \mathcal{E}\hat{\mathbf{x}}e^{-ikz-i\Omega t} + \mathcal{E}'\hat{\mathbf{x}}e^{i\mathbf{k}'\cdot\mathbf{R}-i\Omega' t}) + \text{c.c.}\,, \tag{1}$$

where

$$\mathbf{k} = k\hat{\mathbf{z}},\ \mathbf{k}' = k[\cos(\theta)\hat{\mathbf{z}} + \sin(\theta)\hat{\mathbf{y}}]\,. \tag{2}$$

In this paper, we consider two limiting cases: (i) $\theta \ll 1$, which corresponds to a situation where the probe field and the nearly copropagating cooling field have orthogonal polarizations ($\aleph = \perp$); and (ii) $\pi - \theta \ll 1$, which corresponds to a situation where the probe field and the nearly copropagating cooling field have parallel polarizations ($\aleph = \parallel$). Both cases are analyzed separately below.

We assume a weak-field limit, which is defined as

$$\chi \ll \Gamma, |\Delta|\,, \tag{3}$$

where $\chi = -d\mathcal{E}/4\sqrt{2}\hbar$ is the cooling field Rabi frequency with a reduced atomic dipole moment $d = -er_{eg}$ and $\Delta = \Omega - \omega$ is the detuning of the cooling field from the atomic resonance frequency ω. The weak-field limit is appropriate for achieving optimal sub-Doppler cooling effects. In this limit, the atomic excited-state populations and the electronic coherences can be adiabatically eliminated, and one obtains the reduced generalized optical Bloch equations for the atomic ground-state density matrix only. To first order in the probe field Rabi frequency

$$\chi' = \epsilon\chi\,, \tag{4}$$

where $\epsilon \ll 1$, the effective equation of motion for the ground state density matrix can be written as

$$\dot{\rho} = \frac{1}{i\hbar}[H,\rho] + [\dot{\rho}]_{\text{relax}}\,, \tag{5}$$

where the Hamiltonian H can be written as

$$H = H^{(0)} + \epsilon\{H^{(1)}e^{i\delta t} + [H^{(1)}]^{\dagger}e^{-i\delta t}\}\,, \tag{6}$$

with $\delta = \Omega' - \Omega$. The zeroth order term $H^{(0)}$ is given by

$$H^{(0)} = \frac{\mathbf{p}^2}{2M} + U_0\left[1 + \frac{1}{2}\sin(2kz)\right]|+\rangle\langle+| + U_0\left[1 - \frac{1}{2}\sin(2kz)\right]|-\rangle\langle-|\,, \tag{7}$$

where

$$U_0 = \frac{8}{3}\frac{\Delta\chi^2}{(\Gamma/2)^2 + \Delta^2} \tag{8}$$

is the modulation depth of the light shift potentials. The first order term $H^{(1)}$ is given by

$$H^{(1)} = \frac{U_0}{4}[-ie^{ik[1-\cos(\theta)]z - ik\sin(\theta)y} + 2e^{-ik[1+\cos(\theta)]z - ik\sin(\theta)y}]|+\rangle\langle+| + \frac{U_0}{4}[ie^{ik[1-\cos(\theta)]z - ik\sin(\theta)y} + 2e^{-ik[1+\cos(\theta)]z - ik\sin(\theta)y}]|-\rangle\langle-|\,. \tag{9}$$

In Eqs. (7) and (9), $|\pm\rangle$ denote the ground-state sublevels $|g,\pm 1/2\rangle$, respectively. The term $[\dot{\rho}]_{\text{relax}}$ in Eq. (5) represents the effects of optical pumping on the atomic density matrix evolution, which can be written as

$$[\dot{\rho}]_{\text{relax}} = -\frac{\Gamma'}{2}[A\rho + \rho A] + \Gamma'\int d\mathbf{p}' \sum_{Q=-1}^{1} \times N_Q(\mathbf{p}')B_Q^{\dagger}e^{-i\mathbf{p}'\cdot\mathbf{R}/\hbar}\rho e^{i\mathbf{p}'\cdot\mathbf{R}/\hbar}B_Q\,, \tag{10}$$

where $\Gamma' = \Gamma\chi^2/[(\Gamma/2)^2 + \Delta^2]$ is the optical pumping rate and

$$A = A^{(0)} + \epsilon\{A^{(1)}e^{i\delta t} + [A^{(1)}]^{\dagger}e^{-i\delta t}\}\,, \tag{11}$$

with

$$A^{(0)} = \frac{4}{3}[2 + \sin(2kz)]|+\rangle\langle+| + \frac{4}{3}[2 - \sin(2kz)]|-\rangle\langle-| \tag{12}$$

and

$$A^{(1)} = \frac{2}{3}[-ie^{ik[1-\cos(\theta)]z-ik\sin(\theta)y} +2e^{-ik[1+\cos(\theta)]z-ik\sin(\theta)y}]|+\rangle\langle+| +[ie^{ik[1-\cos(\theta)]z-ik\sin(\theta)y} +2e^{-ik[1+\cos(\theta)]z-ik\sin(\theta)y}]|-\rangle\langle-| . \quad (13)$$

Similarly,

$$B_Q = B_Q^{(0)} + \epsilon\{B_Q^{(1)}e^{i\delta t} + [B_Q^{(1)}]^\dagger e^{-i\delta t}\} , \quad (14)$$

with

$$B_\pm^{(0)} = (-ie^{-ikz} \mp e^{ikz})|\pm\rangle\langle\pm| +\frac{1}{3}(-ie^{-ikz} \mp e^{ikz})|\mp\rangle\langle\mp| ,$$
$$B_0^{(0)} = \frac{\sqrt{2}}{3}(-ie^{-ikz} + e^{ikz})|+\rangle\langle-| +\frac{\sqrt{2}}{3}(-ie^{-ikz} - e^{ikz})|-\rangle\langle+| , \quad (15)$$

and

$$B_\pm^{(1)} = \mp e^{-ik\cos(\theta)z-ik\sin(\theta)y}\left(|\pm\rangle\langle\pm| + \frac{1}{3}|\mp\rangle\langle\mp|\right) ,$$
$$B_0^{(1)} = \frac{\sqrt{2}}{3}e^{-ik\cos(\theta)z-ik\sin(\theta)y}(|+\rangle\langle-| - |-\rangle\langle+|) . \quad (16)$$

The functions $N_{\pm,0}(\mathbf{p}')$ in Eq. (10) are the spontaneous photon momentum distribution functions associated with the σ ($Q = \pm$) or π ($Q = 0$) transitions. As a simplification, we assume that the spontaneous photon momentum $\mathbf{p}'$ is along the $\hat{\mathbf{z}}$ direction only, i.e., $\mathbf{p}' = p'\hat{\mathbf{z}}$, and

$$N_\pm(p') = \frac{3}{8\hbar k}\left(1 + \frac{p'^2}{\hbar^2k^2}\right) ,$$
$$N_0(p') = \frac{3}{4\hbar k}\left(1 - \frac{p'^2}{\hbar^2k^2}\right) . \quad (17)$$

The validity of this simplification as well as the effects related to the true three-dimensional character of the atomic spontaneous emission will be discussed below.

One can accordingly write down the atomic ground-state density matrix ρ as

$$\rho = \rho^{(0)} + \epsilon\{\rho^{(1)}e^{i\delta t} + [\rho^{(1)}]^\dagger e^{-i\delta t}\} . \quad (18)$$

The probe absorption coefficient, excluding the linear absorption term, is found to be given by [4,8]

$$C_{ab} = \mathrm{Im}\left[\frac{\chi}{\Gamma/2 + i\Delta}\langle 2i\rho_s^{(1)}e^{ik[1+\cos(\theta)]z+ik\sin(\theta)y} -\rho_d^{(1)}e^{-ik[1-\cos(\theta)]z+ik\sin(\theta)y}\rangle\right] , \quad (19)$$

where $\langle\,\rangle$ denotes a spatial average and $\rho_s^{(1)}$ and $\rho_d^{(1)}$ represent probe-modulated atomic population and magnetization gratings, which are defined as

$$\rho_s = \langle+|\rho|+\rangle + \langle-|\rho|-\rangle ,$$
$$\rho_d = \langle+|\rho|+\rangle - \langle-|\rho|-\rangle , \quad (20)$$

respectively.

III. CALCULATION OF THE PROBE ABSORPTION SIGNAL

Although the density matrix equation (5) can be solved in any complete basis, it may offer more insight into the results if one chooses to use the eigenstate basis of the unperturbed Hamiltonian H_0, which includes the reactive part of the atom-cooling field interaction and the free motion of atoms in the directions perpendicular to the optical molasses, respectively. Moreover, as shown below, one may be able to invoke a secular approximation in such an energy basis to simplify the calculation tremendously.

The eigenstates of the Hamiltonian H_0 can be written as a product of $|n,q,\mu\rangle|p_y\rangle$, where the Bloch states $|n,q,\mu\rangle$ (n is the band index and q is the Bloch index, $\mu = \pm$) are the eigenstates of

$$H_z^{(0)} = \frac{p_z^2}{2M} + U_+^{(0)}(z)|+\rangle\langle+| + U_-^{(0)}(z)|-\rangle\langle-| \quad (21)$$

with $U_\pm^{(0)}(z) = U_0[1 \pm \frac{1}{2}\sin(2kz)]$, and the plane wave states $|p_y\rangle$ describe the free motion of atoms in the transverse direction, as characterized by the Hamiltonian $H_y^{(0)} = p_y^2/2M$. The atomic motion in the x direction is not interesting in this problem and is ignored. In this product basis, the atomic density matrix elements can be generally written as

$$\rho(n,q,\mu,p_y;n',q',\mu',p_y') = \langle p_y|\langle n,q,\mu|\rho|n',q',\mu'\rangle|p_y'\rangle . \quad (22)$$

In the absence of the probe field, the atomic density matrix can be solved from Eq. (5) by setting $\chi' = 0$. Since the cooling fields are exactly parallel to the z direction, and since we have assumed that spontaneous emissions occur only along the z direction, the transverse atomic motion is not coupled to the atomic motion in the direction of the molasses. As in Refs. [3,4], we assume in this paper a secular approximation defined as

$$|\Delta| \gg \Gamma , \quad (23)$$

which enables us to neglect the off-diagonal density matrix elements in the Bloch state basis. As a result, the only nonvanishing quantities in the Bloch-state space are the populations of various states $\pi_{n,q,\mu}^{(0)}$. The atomic momentum distribution in the direction transverse to the 1D molasses is arbitrary in our model. In the experimental situation of Ref. [1], atoms are first cooled by 3D molasses and then two pairs of cooling beams are switched off to obtain a transient 1D molasses. Therefore it is reasonable for us to assume that the atomic momentum distribution in the transverse direction is given by a function $W(p_y)$, whose width is typical of sub-Doppler temperatures, which is on the order of a few $\hbar k$ for alkali-metal

atoms [9]. Consequently, the atomic density matrix to zeroth order in the probe field strength is given by

$$\rho^{(0)}(n,q,\mu,p_y;n',q',\mu',p_y') = \pi^{(0)}_{n,q,\mu} W(p_y)\delta_{n,n'}\delta_{q,q'}\delta_{\mu,\mu'}\delta(p_y-p_y') \ . \quad (24)$$

The values for $\pi^{(0)}_{n,q,\mu}$ are solved from Eq. (5) in the absence of the probe, as shown in detail in Ref. [3].

As the next step, we then solve for the atomic density matrix to first order in the probe field strength and substitute into Eq. (19) to calculate the probe absorption coefficient. As illustrated in Ref. [4] based on a model in which $\theta = 0$, the probe absorption signal has several sources. One is the Raman resonance signal, which arises from stimulated Raman transitions between discretized motional bands in the molasses direction. Another contribution to the signal comes from the Rayleigh resonances, which can also be understood in terms of two-wave mixing processes involving the probe and the cooling fields. In the following, we analyze the effects related to the misalignment of the probe field propagation direction, which is characterized by the small angle θ or $\pi-\theta$, and investigate the cases when these effects can be negligible and cases when these effects can lead to new types of resonance contributions.

A. Raman signals

We first study the case of $\theta \ll 1$, where the probe and the nearly copropagating cooling field have orthogonal polarizations ($\aleph = \perp$). As can be seen from Eq. (19), the density matrix elements that are responsible for various Raman resonance signals have the form $\rho^{(1)}(n,q,\mu,p_y;n+m,q,\mu,p_y+\hbar k\theta)$, where $m = \pm1,\pm2,\ldots$. The equations for steady-state solutions of these Raman coherences are derived from Eq. (5) as

$$\begin{aligned}
&-\left[\frac{\Gamma'}{2}(\langle n,q,\mu|A^{(0)}|n,q,\mu\rangle + \langle n+m,q,\mu|A^{(0)}|n+m,q,\mu\rangle)\right.\\
&\left.+i\delta + i\omega_{n,q,\mu;n+m,q,\mu} - i\frac{kp_y\theta}{M}\right]\rho^{(1)}(n,q,\mu,p_y;n+m,q,\mu,p_y+\hbar k\theta)\\
&+\Gamma'\sum_{n',q',\mu'}\int dp'\sum_Q N_Q(p')\langle n,q,\mu|(B^{(0)}_Q)^\dagger e^{-ip'z/\hbar}|n',q',\mu'\rangle\\
&\times\langle n'+m,q',\mu'|e^{ip'z/\hbar}B^{(0)}_Q|n+m,q,\mu\rangle\rho^{(1)}(n',q',\mu',p_y;n'+m,q',\mu',p_y+\hbar k\theta)\\
&=\frac{i}{\hbar}\langle n,q,\mu|H^{(1)}|n+m,q,\mu\rangle[\pi^{(0)}_{n+m,q,\mu}W(p_y+\hbar k\theta)-\pi^{(0)}_{n,q,\mu}W(p_y)]\\
&+\frac{\Gamma'}{2}\langle n,q,\mu|A^{(1)}|n+m,q,\mu\rangle[\pi^{(0)}_{n+m,q,\mu}W(p_y+\hbar k\theta)+\pi^{(0)}_{n,q,\mu}W(p_y)]\\
&-\Gamma'\sum_{n',q',\mu'}\int dp'\sum_Q N_Q(p')\langle n,q,\mu|(B^{(0)}_Q)^\dagger e^{-ip'z/\hbar}|n',q',\mu'\rangle\\
&\times\langle n',q',\mu'|e^{ip'z/\hbar}B^{(1)}_Q|n+m,q,\mu\rangle\pi^{(0)}_{n',q',\mu'}W(p_y) \ , \qquad (25)
\end{aligned}$$

where

$$\omega_{n,q,\mu;n+m,q,\mu} = \frac{1}{\hbar}(E_{n,q,\mu}-E_{n+m,q,\mu}) \qquad (26)$$

is the frequency difference between the Bloch states $|n,q,\mu\rangle$ and $|n+m,q,\mu\rangle$. As is evident from Eq. (25), the main modification due to $\theta \neq 0$ is the residual Doppler broadening term $kp_y\theta/M$. Assuming that

$$ku\theta \ll \gamma_{n,q,\mu} = \Gamma'\langle n,q,\mu|A^{(0)}|n,q,\mu\rangle \qquad (27)$$

for all values of $\{n,q,\mu\}$, the residual Doppler broadening can be neglected as compared to the width $\gamma_{n,q,\mu}$ owing to optical pumping effects of the cooling fields. As a result, after integrated over p_y, Eq. (25) becomes identical to the one in Ref. [4], where θ is assumed to be zero.

A characteristic Raman signal due to transitions between $\Delta n = \pm1$ and ±2 states is shown in Fig. 2 for the case of $\aleph = \perp$. The cooling field detuning $\Delta = -10\Gamma$ and the potential depth $|U_0| = 170E_k$, where $E_k = \hbar^2k^2/2M$ is the atomic recoil energy. The probe absorption coefficient is plotted as a function of the dimensionless detuning δ/ω_k, where $\omega_k = E_k/\hbar$ is the atomic recoil frequency. As analyzed in detail in Ref. [4], the widths of the Raman signal ($\Delta n = \pm1$) are smaller than the optical pumping rate $\Gamma'(\approx 6.4\omega_k)$, owing to the Lamb-Dicke effects [10]. The difference between the magnitudes of $\Delta n = \pm1$ resonances and those of $\Delta n = \pm2$ is also related to the spatial localization of atoms in the light shift potential wells.

The case of $\theta' = \pi - \theta \ll 1$ ($\aleph = \parallel$) is very similar to that for $\theta \ll 1$, which becomes evident when one substitutes θ with θ' in Eq. (25). It is interesting to note, however, that although the line shapes of the Raman signals are quite similar in these two cases, the magnitude of the signal is approximately a factor of 4 smaller in the case of $\pi - \theta \ll 1$ ($\aleph = \parallel$) than in the case of $\theta \ll 1$

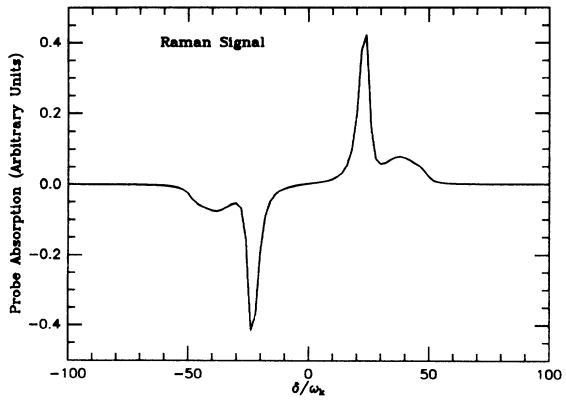

FIG. 2. Raman resonance signal in the case of $\aleph = \perp$. $\Delta = -10\Gamma$, and the potential depth $|U_0| = 170.5E_k$.

($\aleph = \perp$). Such a difference is due to the factors of 2 in both the Hamiltonian (9) and the signal expression (19), which in turn are due to the interference between signals originating from $|m = \pm 1/2\rangle \rightarrow |m = \pm 3/2\rangle$ and $|m = \pm 1/2\rangle \rightarrow |m = \mp 1/2\rangle$ transitions, respectively. In the case of a $F \rightarrow F+1$ transition, where $F \geq 1$, the difference between the transition strengths of $|m = \pm F\rangle \rightarrow |m = \pm F \pm 1\rangle$ and $|m = \pm F\rangle \rightarrow |m = \pm F \mp 1\rangle$ becomes greater, and one expects the magnitudes of the Raman signals in these two cases to approach each other.

B. Central resonances at $\delta = 0$

We now discuss the contributions to the resonance line shapes at $\delta = 0$, which have been previously attributed to some Rayleigh processes involving the probe and the cooling fields [4]. As shown below, there is another type of processes that can contribute to the narrow signal at $\delta = 0$.

As shown in Ref. [4], it is helpful to use the so-called adiabatic states, or the eigenstates of the Hamiltonian H, to evaluate the probe-modified density matrix elements that leads to the central signal. The adiabatic states are derived from first order perturbation theory as

$$\overline{|n,q,\mu\rangle} = |n,q,\mu\rangle + \epsilon[|n,q,\mu\rangle_+^{(1)} e^{i\delta t} + |n,q,\mu\rangle_-^{(1)} e^{-i\delta t}] , \tag{28}$$

where

$$|n,q,\mu\rangle_+^{(1)} = \sum_{n'(\neq n)} \frac{\langle n',q,\mu|H^{(1)}|n,q,\mu\rangle}{E_{n,q} - E_{n',q}} |n',q,\mu\rangle ,$$

$$|n,q,\mu\rangle_-^{(1)} = \sum_{n'(\neq n)} \frac{\langle n',q,\mu|[H^{(1)}]^\dagger|n,q,\mu\rangle}{E_{n,q} - E_{n',q}} |n',q,\mu\rangle . \tag{29}$$

Notice that the coefficients of $|n,q,\mu\rangle_\pm^{(1)}$ are still operators for the atomic motion in y direction. Under the secular approximation (3), and from Eq. (19), one calculate the probe-modulated density matrix elements of form

$$\bar{\pi}_{n,q,\mu}^{(1)}[p_y, p_y + \hbar k \sin(\theta)]$$

$$= \langle p_y|\overline{\langle n,q,\mu|}\rho^{(1)}\overline{|n,q,\mu\rangle}|p_y + \hbar k \sin(\theta)\rangle , \tag{30}$$

which leads to the central structures of the probe absorption signal. The equation for the equilibrium values of $\bar{\pi}_{n,q,\mu}^{(1)}[p_y, p_y + \hbar k \sin(\theta)]$ is given by

$$\begin{aligned}
&-\left[\gamma_{n,q,\mu} + i\delta - i\frac{kp_y \sin(\theta)}{M}\right] \bar{\pi}_{n,q,\mu}^{(1)}[p_y, p_y + \hbar k \sin(\theta)] \\
&+\Gamma' \sum_{n',q',\mu'} \int dp' \sum_Q N_Q(p') |\langle n',q',\mu'|e^{ip'z/\hbar} B_Q^{(0)}|n,q,\mu\rangle|^2 \bar{\pi}_{n',q',\mu'}^{(1)}[p_y, p_y + \hbar k \sin(\theta)] \\
&= -\frac{i}{\hbar}\langle n,q,\mu|H^{(1)}|n,q,\mu\rangle \bar{\pi}_{n,q,\mu}^{(0)}\{W(p_y) - W[p_y + \hbar k \sin(\theta)]\} \\
&\quad +\frac{1}{2}\Gamma'\langle n,q,\mu|A^{(1)}|n,q,\mu\rangle \bar{\pi}_{n,q,\mu}^{(0)}\{W(p_y) + W[p_y + \hbar k \sin(\theta)]\} \\
&\quad +\Gamma'[{}_-^{(1)}\langle n,q,\mu|A^{(0)}|n,q,\mu\rangle W[p_y + \hbar k \sin(\theta)] + \langle n,q,\mu|A^{(0)}|n,q,\mu\rangle_+^{(1)} W(p_y)] \bar{\pi}_{n,q,\mu}^{(0)} \\
&\quad -\Gamma' \sum_{n',q',\mu'} \int dp' \sum_Q N_Q(p') \langle n,q,\mu|(B_Q^{(0)})^\dagger e^{-ip'z/\hbar}|n',q',\mu'\rangle \langle n',q',\mu'|e^{ip'z/\hbar} B_Q^{(1)}|n,q,\mu\rangle \bar{\pi}_{n',q',\mu'}^{(0)} W(p_y) \\
&\quad -\Gamma' \sum_{n',q',\mu'} \int dp' \sum_Q N_Q(p') {}_-^{(1)}\langle n,q,\mu|(B_Q^{(0)})^\dagger e^{-ip'z/\hbar}|n',q',\mu'\rangle \langle n',q',\mu'|e^{ip'z/\hbar} B_Q^{(0)}|n,q,\mu\rangle \bar{\pi}_{n',q',\mu'}^{(0)} W[p_y + \hbar k \sin(\theta)] \\
&\quad -\Gamma' \sum_{n',q',\mu'} \int dp' \sum_Q N_Q(p') \langle n,q,\mu|(B_Q^{(0)})^\dagger e^{-ip'z/\hbar}|n',q',\mu'\rangle_+^{(1)} \langle n',q',\mu'|e^{ip'z/\hbar} B_Q^{(0)}|n,q,\mu\rangle \bar{\pi}_{n',q',\mu'}^{(0)} W[p_y + \hbar k \sin(\theta)] \\
&\quad -\Gamma' \sum_{n',q',\mu'} \int dp' \sum_Q N_Q(p') \langle n,q,\mu|(B_Q^{(0)})^\dagger e^{-ip'z/\hbar}|n',q',\mu'\rangle_-^{(1)} \langle n',q',\mu'|e^{ip'z/\hbar} B_Q^{(0)}|n,q,\mu\rangle \bar{\pi}_{n',q',\mu'}^{(0)} W(p_y) \\
&\quad -\Gamma' \sum_{n'} \int dp' \sum_Q N_Q(p') \langle n,q,\mu|(B_Q^{(0)})^\dagger e^{-ip'z/\hbar}|n',q',\mu'\rangle \langle n',q',\mu'|e^{ip'z/\hbar} B_Q^{(0)}|n,q,\mu\rangle_+^{(1)} \bar{\pi}_{n',q',\mu'}^{(0)} W(p_y) .
\end{aligned} \tag{31}$$

In the following, we study the cases of (i) $\theta \ll 1$ ($\aleph = \perp$) and (i) $\pi - \theta \ll 1$ ($\aleph = \parallel$), separately.

1. Case of $\theta \ll 1$

To first order in θ, one has $\sin(\theta) = \theta$ and $\cos(\theta) = 1$. Based on Eq. (19), the central signal depends on the momentum integral of the density matrix elements

$$\int \bar{\pi}^{(1)}_{n,q,\mu}(p_y, p_y + \hbar k\theta) dp_y \ .$$

Since we assume that the residual Doppler width $ku\theta$ is much smaller than any relaxation rate of the Bloch state [see (27)], we can neglect the transverse Doppler broadening term $kp_y\theta/M$ in Eq. (31). After one integrates Eq. (31) over p_y, the dependence of Eq. (31) on θ vanishes and we recover the same equation in Ref. [4] when θ is taken to be exactly zero. The resulting signal is entirely due to Rayleigh-type transitions between the Bloch states in the molasses direction. A typical central line shape is shown in Fig. 3 for the case of $\aleph = \perp$. The signal is a superposition of the back-scattering contribution related to the population grating $\rho^{(1)}_s$ (which has a spatial period of $\lambda/2$) and forward-scattering contribution related to a global magnetization $\rho^{(1)}_d$. Since the back-scattering part is primarily related to the lowest motional states in the molasses [4], it has a narrower linewidth as compared with the forward-scattering term, to which all motional bands contribute. As a result, the overall line shape exhibits a clifflike feature at $\delta = 0$.

2. Case of $\pi - \theta \ll 1$

To first order in $\theta' = \pi - \theta$, one has $\sin(\theta) = \theta'$ and $\cos(\theta) = -1$. One might think it is possible to similarly eliminate the dependence of Eq. (31) on θ' by assuming that

$$ku\theta' \ll \gamma_{n,q,\mu} \ , \tag{32}$$

and integrate Eq. (31) over p_y. Following this procedure, one finds that the population term $\langle \rho^{(1)}_s \rangle$ in Eq. (19) is exactly zero, as required by conservation of population. This is also evident from Eq. (31). After eliminating the transverse momentum p_y from Eq. (31), it is easy to show that the sum $\sum_{n,q,\mu} \bar{\pi}^{(1)}_{n,q,\mu}$ is indeed zero. As a result, the only Rayleigh contribution to the central signal at $\delta = 0$ comes from the magnetization grating term $\rho^{(1)}_d$, which represents the backscattering of the cooling field into the probe field. Figure 4(a) shows the line shape of this Rayleigh signal due to such a backscattering process for the case of a "deep" potential well ($|U_0| = 170E_k$). Notice that the sign of the dispersion is the reverse of the experimental curve shown in Ref. [1]. As pointed out in Ref. [4], and also confirmed by the present calculation, the sign of this dispersion reverses when one chooses a "shallow" potential well (with $|U_0|$ typically of order $10E_k$). The fact that such a sign reversal has not been found in experiments so far constitutes a major discrepancy between the existing theory and the experiments [11].

In the following, we show that when the transverse broadening is included, the sum of

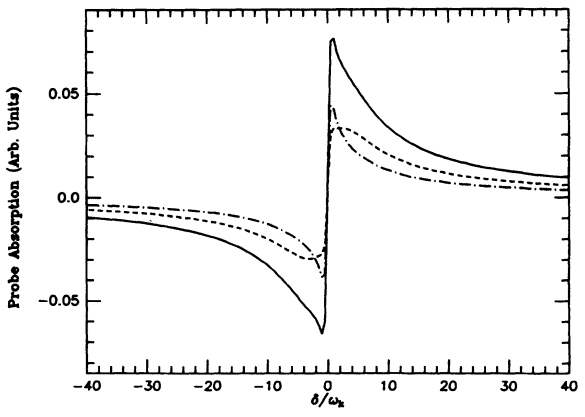

FIG. 3. Rayleigh resonance signal in the case of $\aleph = \perp$. Cooling field parameters are the same as in Fig. 2. Dot-dashed line represents the back-scattering contribution, dashed line the forward-scattering contribution, and solid line the overall signal.

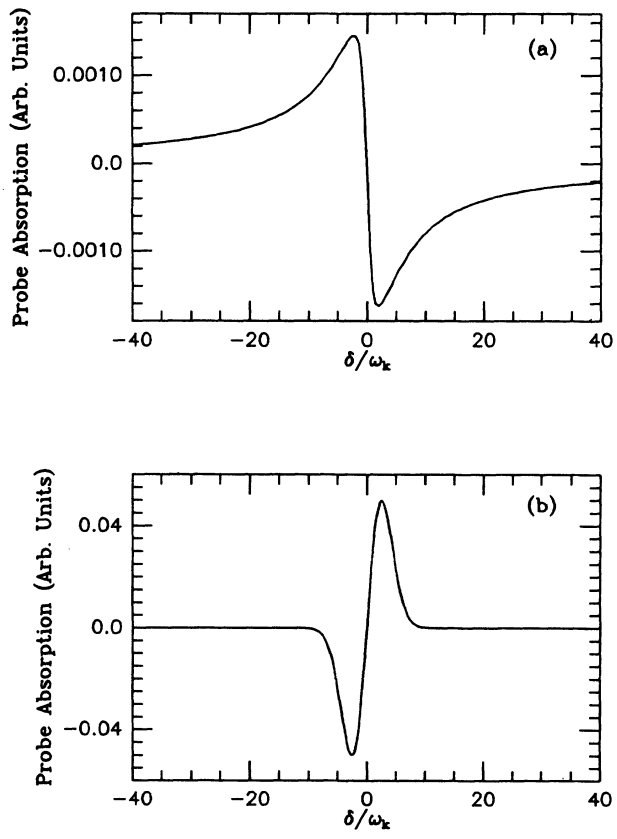

FIG. 4. Central resonance signal in the case of $\aleph = \parallel$. The cooling field parameters are the same as in Fig. 2. (a) Rayleigh signal due to back-scattering processes. (b) Recoil-induced signal. The most probable transverse momentum $Mu = 18\hbar k$.

$$\int \sum_{n,q,\mu} \bar{\pi}^{(1)}_{n,q,\mu}(p_y, p_y + \hbar k\theta')dp_y \ , \tag{33}$$

which represents a population grating in the y direction with a grating period λ/θ', does lead to an important contribution to the probe absorption signal. Such a contribution originates from the recoil-induced resonances between atomic states with different transverse momentum p_y.

One may ask the following question: why in one case ($\aleph = \perp$) it is possible to neglect the transverse broadening $kp_y\theta/M$, while in the other ($\aleph = \|$) it is not, although one assumes in both cases the same condition (27) or (32). The answer lies in the following. In the case of $\aleph = \perp$, the population modification in each Bloch state, i.e., $\bar{\pi}^{(1)}_{n,q,\mu}$, contributes to the Rayleigh signal independently, owing to the fact that the signal (19) depends on the average of the product $\langle \rho^{(1)}_s e^{2ikz} \rangle$. Since the average values of e^{2ikz} for different Bloch states are different, the inclusion of the residual Doppler broadening has negligible modification for the sum $\sum_{n,q,\mu} \bar{\pi}^{(1)}_{n,q,\mu'} \langle n,q,\mu|e^{2ikz}|n,q,\mu\rangle$ under condition (27). In the case of $\aleph = \|$, however, the signal depends on the sum of the modified population $\langle \rho^{(1)}_s \rangle$ itself, which is exactly zero if one assumes the misalignment angle $\theta' = 0$. In fact, optical pumping does not induce any decay of the sum of the population modifications of all Bloch states $\sum_{n,q,\mu} \bar{\pi}^{(1)}_{n,q,\mu}$. Thereby the condition (32) under which transverse broadening can be neglected is not applicable for the modified total population. When the finite angle θ' is taken into consideration, the summation (33) no longer gives zero signal. In fact, it represents the contribution of the recoil-induced resonances in the transverse degree of freedom.

To obtain the expression for the recoil-induced signal, one needs the evolution equation for the coherence between atomic states with different c.m. momenta

$$\rho^{(1)}(p_y, p_y + \hbar k\theta') = \sum_{n,q,\mu} \bar{\pi}^{(1)}_{n,q,\mu}(p_y, p_y + \hbar k\theta') \ . \tag{34}$$

Starting from Eq. (5), and in a similar procedure that leads to Eq. (31), we obtain the equation of motion for $\rho^{(1)}(p_y, p_y + \hbar k\theta')$ as

$$\begin{aligned} &\dot{\rho}^{(1)}(p_y, p_y + \hbar k\theta') \\ &\quad = -\left(\gamma_t + i\delta - i\frac{kp_y\theta'}{M}\right)\rho^{(1)}(p_y, p_y + \hbar k\theta') \\ &\qquad -\frac{i}{\hbar}\left[\sum_{n,q,\mu} \langle n,q,\mu|H^{(1)}|n,q,\mu\rangle \pi^{(0)}_{n,q,\mu}\right] \\ &\qquad \times [W(p_y + \hbar k\theta') - W(p_y)] \ , \end{aligned} \tag{35}$$

where we have kept only the source term to lowest order in $\Gamma'/|U_0|$ under the secular approximation (3). In the above equation, γ_t is an added effective decay rate, which is assumed to be much smaller than any relevant linewidth in this problem (e.g., $ku\theta'$). It can be determined, for example, by the transit time of atoms in the laser fields [12]. The source term on the right-hand side of Eq. (35) is proportional to the difference of populations between atomic states of transverse momentum p_y and $p_y + \hbar k\theta$, which is characteristic of the recoil-induced signal [7,8]. The steady-state solution for $\rho^{(1)}(p_y, p_y + \hbar k\theta')$ can be easily obtained from Eq. (35), and one finds the contribution of the recoil-induced resonances to the probe absorption signal (19) as

$$\begin{aligned} C^{(\mathrm{RIR})}_{ab} &= \mathrm{Im}\left[\frac{2i\chi}{\Gamma/2 + i\Delta}\langle \rho^{(1)}_s e^{ik\theta' y}\rangle\right] \\ &= \mathrm{Im}\left[\frac{2i\chi}{\Gamma/2 + i\Delta}\int dp_y \rho^{(1)}(p_y, p_y + \hbar k\theta')\right] \\ &= \mathrm{Im}\left\{\frac{\pi\chi}{\Gamma/2 + i\Delta} MU_0 W'\left(\frac{M\delta}{k\theta'}\right)\right. \\ &\quad \left.\times\left[2 - i\sum_{n,q}(\langle n,q,+|e^{i2kz}|n,q,+\rangle \pi^{(0)}_{n,q,+} - \langle n,q,-|e^{2ikz}|n,q,-\rangle \pi^{(0)}_{n,q,-})\right]\right\} \ , \end{aligned} \tag{36}$$

where $W'(p_y)$ is the first order derivative of $W(p_y)$ with respect to p_y. As we mentioned earlier, the atomic transverse momentum distribution $W(p_y)$ is arbitrary in our model. If we assume $W(p_y)$ to be a Gaussian distribution with a width $p_0 = Mu$, i.e.,

$$W(p_y) = \frac{1}{\sqrt{\pi}p_0}\exp\left(-\frac{p_y^2}{p_0^2}\right) \ , \tag{37}$$

then the dependence of the recoil-induced signal on the probe-pump detuning δ has the following form:

$$C^{(\mathrm{RIR})}_{ab} \propto \frac{U_0}{\hbar\Delta}\frac{\chi\omega_k}{(ku)^2}\frac{\delta}{ku\theta'}\exp\left[\frac{\delta^2}{(ku\theta')^2}\right] \ . \tag{38}$$

As one can see from the above expression, the recoil-induced signal appears to be a Gaussian-type dispersion, with probe gain for negative δ ($C_{ab} < 0$) and probe loss for positive δ ($C_{ab} > 0$). The peak-to-peak distance is given by $\sqrt{2}ku\theta'$. The magnitude of RIR signal is determined by the factor $[U_0/(\hbar\Delta)][\chi\omega_k/(ku)^2]$, which can be compared to other signals due to, for example, the Rayleigh resonances. Figure 4(b) shows the RIR signal (36) for a potential depth $|U_0|/E_k = 170$ and a transverse momentum width $Mu = 18\hbar k$, which corresponds to a temperature $T_\perp = 1/2Mp_y^2$ of order 60 μK for cesium atoms. As one can see from Figs. 4(a) and 4(b), which are drawn using the same unit, the recoil-induced signal (b) has a much greater amplitude for this transverse tem-

perature than the signal (a) due to Rayleigh resonances, and it has the same sign as the experimental curve shown in Ref. [1]. Based on Eq. (38), as ku increases, the width of the RIR signal increases linearly as $ku\theta'$ and its magnitude decreases quadratically as $1/(ku)^2$. These features serve as evidence of RIR.

So far we have assumed that spontaneous emissions occur only in the molasses direction [see Eq. (17)]. In reality, spontaneous photons can be emitted into the transverse directions as well, which constitutes a diffusive heating mechanism due to the random directions of spontaneous photons. To lowest order in $\Gamma/|\Delta|$, the recoil-induced signal is independent of the spontaneous decay pattern [7]. However, the transverse momentum width $p_0 = Mu$ is now a function of time, roughly given by

$$p_0(t) = \sqrt{\sigma_0^2 + D_\perp t}\,, \tag{39}$$

where σ_0 is the initial momentum width at $t = 0$ and $D_\perp$ is the transverse momentum diffusion constant. If we assume that the rate of change of p_0 is much smaller than the residual Doppler width $ku\theta'$, our calculation of RIR is still valid. The resulting line shape of the recoil-induced signal follows the evolution of $p_0(t)$ adiabatically and its width increases with time as $ku(t)\theta'$.

IV. CONCLUSIONS

We have presented a calculation of the probe-absorption coefficient for atoms cooled in 1D optical molasses. Unlike the treatment in Ref. [4], we allow a small misalignment of the probe characterized by the angle θ between the probe and the cooling-field propagation directions. The effects related to such a misalignment are analyzed. The results can be summarized as follows.

(a) For the signal originating from stimulated Raman transitions between the quantized motional states (Bloch states) along the molasses direction, which appears as sidebands in the probe absorption spectra, the misalignment leads to a small broadening of the Raman signal by the residual Doppler width $ku\sin(\theta)$, which can be neglected when $ku\sin(\theta)$ is much smaller than the effective relaxation rates $\gamma_{n,q,\mu}$ of the Bloch states involved in the transitions.

(b) For the central signal at $\delta = 0$, we have addressed two different situations.

(i) For $\aleph = \perp$, which represents the case when the probe and the nearly copropagating cooling field have orthogonal polarizations, the effects of the small misalignment can still be neglected under the same assumption that $ku\sin(\theta) \ll \gamma_{n,q,\mu}$ for all Bloch states $|n,q,\mu\rangle$. The signal constitutes both a forward-scattering and a backscattering contribution (Rayleigh signal), which appears as a cliff-shaped dispersion.

(ii) For $\aleph = \|$, which represents the case when the probe and the nearly copropagating cooling field have parallel polarizations, one can no longer neglect the misalignment effects when considering the signal related to the population term $\rho_s^{(1)}$. Our calculation shows that this misalignment leads to an additional signal due to the recoil-induced processes between the transverse energy continuum states. The magnitude of this recoil-induced signal can be much greater than the Rayleigh signal previously studied, and its sign is independent of the depth of the optical potential wells in the molasses direction.

Some recent 1D probe transmission experiments without the transverse confining beams [13] have confirmed that the narrow central resonance structure observed in the $\aleph = \|$ case indeed fits very well into a derivative of a Gaussian of form (38) and its sign does not change for different signs and magnitudes of U_0. Perhaps more interesting is that the width of the dispersion increases with the time delay between the shutdown of transverse cooling beams and the turn on of the probe beam, which agrees with the arguments above concerning the effects of transverse heating due to spontaneous emissions. All these new developments lead one to believe that the narrow central line shape in this case is indeed the recoil-induced resonances related to the transverse degree of freedom. If so, this will be the first observation of the recoil-induced resonances proposed initially for two-level atoms [7]. The determination of the width of the RIR signal as a function of time constitutes a measurement of the transverse momentum diffusion rate $D_\perp$, which may be compared with results of theoretical calculations.

ACKNOWLEDGMENTS

I would like to thank P. R. Berman and G. Grynberg for helpful discussions. This research is supported by the National Science Foundation Grant No. PHY 9113590.

[1] P. Verkerk, B. Lounis, C. Salomon, C. Cohen-Tannoudji, J.-Y. Courtois, and G. Grynberg, Phys. Rev. Lett. **68**, 3861 (1992).

[2] P. Jessen, C. Gerz, P. D. Lett, W. D. Phillips, S. L. Rolston, R. J. C. Spreeuw, and C. I. Westbrook, Phys. Rev. Lett. **69**, 49 (1992).

[3] Y. Castin and J. Dalibard, Europhys. Lett. **14**, 761 (1991).

[4] J.-Y. Courtois and G. Grynberg, Phys. Rev. A **46**, 7060 (1992).

[5] P. Marte, R. Dum, R. Tàieb, and P. Zoller, Phys. Rev. A **47**, 1378 (1993).

[6] G. Grynberg, M. Vallet, and M. Pinard, Phys. Rev. Lett. **65**, 701 (1990).

[7] J. Guo, P. R. Berman, B. Dubetsky, and G. Grynberg, Phys. Rev. A **46**, 1426 (1992).

[8] J. Guo and P. R. Berman, Phys. Rev. A **47**, 4128 (1993).

[9] We neglect the spatial modulation of the atomic density matrix induced by the initial transverse cooling fields, assuming that any initial coherences between transverse atomic external degrees of freedom are damped out by momentum diffusion associated with 3D atomic sponta-

neous emissions before the probe field is turned on.
[10] R. Dicke, Phys. Rev. **89**, 472 (1953).
[11] G. Grynberg (private communication).
[12] Alternatively, one can integrate Eq. (35) without the decay term γ_t. In the limit that γ_t is much smaller than the residual Doppler width $ku\theta'$, these two approaches give the same results. For more detail, see B. Dubetsky and P. R. Berman, Phys. Rev. A **47**, 1294 (1993).
[13] J.-Y. Courtois, G. Grynberg, B. Lounis, and P. Verkerk (unpublished). We are grateful to these authors for sending us their results prior to publication.